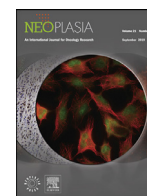




ELSEVIER

Contents lists available at ScienceDirect

Neoplasia

journal homepage: www.elsevier.com/locate/neo

A trio of tumor suppressor miRNA downregulates CREB5 dependent transcription to modulate neoadjuvant hormonal therapy sensitivity

Xueli Wang^{a,b,1}, Bo Han^{b,c,1}, Baokai Dou^d, Lin Gao^b, Feifei Sun^b, Mei Qi^c, Jing Zhang^{d,*},
Jing Hu^{c,*}

^a Department of Pathology, Binzhou City Central Hospital, Binzhou 251700, China

^b The Key Laboratory of Experimental Teratology, Ministry of Education and Department of Pathology, School of Basic Medical Sciences, Cheeloo College of Medicine, Shandong University, Jinan, Shandong 250012, China

^c Department of Pathology, Qilu Hospital, Cheeloo College of Medicine, Shandong University, Jinan, Shandong 250012, China

^d Department of Pharmacy, Shandong Provincial Hospital Affiliated to Shandong First Medical University, Jinan, Shandong 250021, China



ARTICLE INFO

Keywords:

miRNA
CREB5
Prostate cancer
Neoadjuvant hormonal therapy
Bicalutamide

ABSTRACT

Neoadjuvant hormonal therapy (NHT) prior to radical prostatectomy (RP) is an approach that can potentially maximize survival outcomes in prostate cancer (PCa) patients with high-risk disease. Unfortunately, subsets of patients do not respond well to such hormonal therapy. We previously identified several pathological parameters in predicting differences in response to NHT of PCa. However, little is known about the potential role and mechanism of miRNAs mediated NHT resistance (NHT-R) in PCa. Here we demonstrate that miR-142-3p, miR-150-5p and miR-342-3p are the top downregulated miRNAs in PCa tissues with NHT-R. Functional analysis reveals that the three miRNAs inhibit cell proliferation *in vitro*. Transfection of miRNAs mimics strengthens the inhibitory effects of bicalutamide and enzalutamide to PCa cells. Luciferase reporter assay reveals that CREB5 is the common target of these three miRNAs. Clinically, high expression level of CREB5 correlates with high Gleason score, advanced tumor stage and NHT-R in PCa tissues. CREB5 expression promotes antiandrogen therapy resistance in LNCaP cells and IL6 signaling pathway may be involved in this process. In all, our findings highlight an important role of miR-142-3p, miR-150-5p, and miR-342-3p in contributing NHT-R by targeting CREB5 in PCa.

Introduction

Neoadjuvant hormonal therapy (NHT) is defined as neoadjuvant androgen blockage therapy that is administered before radical prostatectomy (RP) or radiotherapy (RT). NHT has shown a beneficial effect in lowering the pathologic T stage, decreasing the number of positive lymph node and positive surgical margin rate [1], especially in patients with localized high risk prostate cancer (HRPCa) [2–8]. Unfortunately, subsets of patients do not respond well to such hormonal therapy. Resistance mechanisms against hormonal therapy have already been described, including androgen receptor (AR)-based mutations, alterations in the PTEN–PI3K–Akt pathway, and mutations in DNA damage repair genes [9]. By contrast, possible resistance mechanisms to NHT before RP in HRPCa are unclear. Previously, we have quantified the tumor response to NHT with a new proposed pathological grading system and identified several pathological parameters in predicting response of NHT [10].

MicroRNAs (MiRNAs) are a class of small endogenously expressed non-coding RNAs, which play important roles in cell development, differentiation, proliferation, apoptosis, cancer invasion and metastasis [11]. Over the past decades, a number of studies have highlighted the role of dysregulated miRNAs in driving drug resistance [12,13]. Fattore et al. reported that reprogramming miRNAs global expression is the central cascade of targeted therapy resistance in BRAF-mutated metastatic melanoma by alteration of cell intrinsic proliferation and survival pathways [14]. In breast cancer, miR-489 has been shown to reverse chemotherapy resistance and induce drug related apoptosis via the PI3K/Akt pathway by targeting SPIN1 [15]. In PCa, multiple studies have demonstrated aberrant expression of miRNAs, such as miR-346, miR-361-3p and miR-197 [16], modulate antiandrogen resistance in castration resistant prostate cancer (CRPC) by targeting the AR signaling pathways [17–22]. Previously, we revealed the role of miR-30a induced cell cycle modulation and miR-17-92 cluster related neuroendocrine differentiation in castration-resistant development [23,24]. However, little

* Corresponding authors.

E-mail addresses: 15168889882@163.com (J. Zhang), 201420420@mail.sdu.edu.cn (J. Hu).

¹ These authors contributed equally to this work.

is known about the mechanism of miRNAs in modulating NHT resistance (NHT-R) of PCa. A better understanding of NHT-R mechanisms is important to improve stratification of PCa patient who receive NHT therapeutic strategies.

The gene cAMP responsive element binding protein 5 (CREB5), a transcription factor, has been shown to be upregulated in a series of malignances, including carcinoma of the kidney, ovary, liver, etc. In addition, amplification and overexpression of CREB5 promotes CRPC though significant transcriptomic reprogramming of AR with FOXA1 required [25,26]. In the current study, we show for the first time that miR-142-3p, miR-150-5p and miR-342-3p might play an important role in localized HRPCa with NHT-R. These three miRNAs may modulate NHT sensitivity through targeting CREB5.

Materials and methods

Patients

The clinicopathological data of this study was described as previously [10]. In brief, a total of 85 locally HRPCa patients with matched pairs of diagnostic needle biopsies and RP specimens were included. All patients received preoperative NHT (Leuprorelin/Goserelin + bicalutamide) for at least 3 months. According to our previously grading system criteria, all patients were categorized into 5 groups from Grade 0-4. Patients with Grade 0-1 were considered as NHT-R group and Grade 2-4 as NHT sensitive (NHT-S) group. NHT-R patients were defined as no response or less than 30% reduction of tumor cellularity in residual disease by comparing with pretreatment needle biopsies. This study was approved by Shandong University Medical Research Ethics Committee and informed consent was obtained from each patient.

MicroRNA microarray, mRNA profiling and bioinformatics analysis

Ten pre-NHT needle biopsy samples were used for microarray profile. Agilent Human miRNA Microarray chips (Agilent, California, USA) analysis was performed on 5 PCa cases with NHT-R and 5 cases with NHT-S as previously described [27]. mRNA microarray profiling (Kangcheng, Shanghai, China) was used to compare the mRNA expression in LNCaP cells upon CREB5 overexpression. The microarray data were deposited into the NCBI's Gene Expression Omnibus (GEO) Repository (<http://www.ncbi.nlm.nih.gov/geo>) and are now accessible through GEO series accession number GSE186994 and GSE186380, respectively. The Cancer Genome Atlas (TCGA) datasets were downloaded from (<http://gdac.broadinstitute.org/>). Datasets of GSE21032, GSE116918 and GSE141551 were downloaded from the Gene Expression Omnibus (GEO) database (<http://www.ncbi.nlm.nih.gov/geo>). The expressed genes were analyzed for enrichment of biological themes using Gene Set Enrichment Analysis (GSEA) (<http://software.broadinstitute.org/gsea/index.jsp>). Enrichment score of miRNAs targets signatures and AR related signatures were quantified by ssGSEA in R package GSVA. The signatures were downloaded from molecular signature database of GSEA (<https://www.gsea-msigdb.org/gsea/msigdb/index.jsp>).

Cell culture and reagents

Human PCa cell lines LNCaP, VCaP, 22RV1, C4-2B and HEK-293T were obtained from the American Type Culture Collection (Rockville, MD, USA) and cultured following ATCC's instructions. Cells were authenticated again by short tandem repeat analysis before our study. The enzalutamide-resistant cell line LNCaP-ENZR was established as previously described [28]. In the relevant experiments of bicalutamide or enzalutamide, charcoal-stripped fetal bovine serum medium (CS-FBS) was used. Cells were all cultured at 37°C with 5% CO₂. Enzalutamide (HY-70002, Med Chem Express) and bicalutamide (B803285, Mack Lin) were prepared according to the manufacturers' instructions.

Plasmids and cell transfection

CREB5 (Gene ID: 9586; [NM_001011666.3](https://www.ncbi.nlm.nih.gov/nuccore/NM_001011666.3), vector: pENTER) cDNA expression vectors were designed and synthesized by GenePharma (Shanghai, China). siRNA against CREB5 (5'-CCAGCAUAAUACCAUCACUTT-3'), and miR-142-3p, miR-150-5p, miR-342-3p mimics/inhibitor, and the respective negative controls were purchased from GenePharma (Shanghai, China). The sequence of the three miRNA mimics/inhibitor and the negative control were shown in Table S1. Lipofectamine 3000 (Invitrogen, Carlsbad, CA) was used for transfection following the manufacturer's instruction. The effect of transfection efficiency was confirmed using quantitative real-time PCR (RT-qPCR) and Western blot assay.

RNA isolation and RT-qPCR assays

Total RNA was extracted with Trizol reagents (Invitrogen, Carlsbad, CA) following the manufacturer's instructions. MiRNA was extracted according to the manufacturer's instruction of high pure miRNeasy FFPE Kit (Bioteke, Beijing, China). ReverTra Ace qPCR RT kit and SYBR Green PCR kit (Toyobo, Japan) were used to examine the mRNA levels (TOYOBO, Japan). GAPDH was used as an internal loading control for mRNA. Pre-U6 was used as an endogenous control for pre-miRNA. For detecting mature miRNA, RT-qPCR assay was performed using All-in-One miRNA qRT-PCR Detection Kit (GeneCopoeia, USA). The sequence of primers used are shown in Table S2.

In vitro proliferation and colony formation assays

Assays were performed according to the protocols as previously described [28,29]. Cell proliferation was measured by EdU assays (Ribobio, Guangzhou, China), 3-(4,5-dimethylthiazol-2-yl)-5-(3-carboxymethoxyphenyl)-2-(4-sulfophenyl)-2H-tetrazolium inner salt (MTS) assays (Promega, Madison, WI, USA) or colony formation assays according to the manufacturer's protocol. For colony formation assays, cells were cultured for two weeks followed by staining with crystal violet and photography. Colonies containing more than 50 cells are counted and plotted.

Dual luciferase assay

Dual luciferase assay was performed as previously described [30]. HEK-293T cells were used to perform the luciferase assay. The wild and mutant potential recognizing regions of miR-142-3p, miR-150-5p, miR-342-3p in 3'UTR region of CREB5 were subcloned into pmirGLO vector (GenePharma, Shanghai, China), respectively. HEK-293T cells were transiently transfected with reporter constructs together with miRNA mimics and the corresponding control using Tuberfect transfection reagent (Thermo). Cells were lysed at 48h after transfection. Dual luciferase assay reporter system was carried out according to the manufacturer's instructions (Promega).

Western blot

Western blot analysis was performed as previously described [31]. The membranes were incubated overnight with antibodies against CREB5 (G420, 1:300, Santa Cruz) and GAPDH (1:1000, Santa Cruz). Immunoreactivity was visualized using an enhanced chemiluminescence kit (Millipore, Darmstadt, Germany).

Tissue microarray (TMA) construction and Immunohistochemistry (IHC)

Two TMAs were constructed using 1.0 mm cores and IHC was performed as previously described [32]. Briefly, sections were incubated overnight with primary antibody against CREB5 (Abnova, 8A5, USA, 1:300) at 4 °C. The slides were evaluated blindly by two independent

observers (X.W. and B.H.). CREB5 expression was divided into two categories according to the nucleus staining intensity, negative (no staining) or weakly positive (only visible at high magnification); moderately (visible at low magnification) or strongly positive (striking at low magnification).

Statistics

Statistical analysis was carried out using SPSS 20.0 or GraphPad prism 8.0 software. With $P < 0.05$ being considered statistically significant. Two-sided Student's t test was used for two groups, one-way analysis of variance was used for statistical comparisons of three or more groups. Receiver-operating characteristic (ROC) curve was dotted to evaluate the diagnostic testing parameters. Correlation significance was assessed using χ^2 and Fisher exact test. Figure legends specify the statistical analysis method performed.

Results

Characteristics of human subjects

The clinicopathological characteristics of 85 PCa cases with preoperative needle biopsies and matched RP specimens were described previously [10]. In brief, 62 out of 85 (73%) PCa cases were of NHT-S, whereas 23 out of 85 (27%) patients were of NHT-R. Representative morphological images of patients with NHT-S or NHT-R in RP specimens were shown in Fig. 1A.

miR-142-3p, miR-150-5p and miR-342-3p are downregulated in NHT-R PCa tissues and correlated with high Gleason score

To search for potential miRNAs that are involved in NHT-R in PCa, the expression levels of 1205 miRNAs were examined by microarray profile using needle biopsy samples from 10 PCa patients with NHT treatment before RP. Forty-three differentially expressed miRNAs were identified between NHT-S ($N = 5$) and NHT-R ($N = 5$) tissues (Fig. 1B), of which 24 miRNAs were significantly upregulated, while the other 19 miRNAs were significantly downregulated in NHT-R tissues compared to NHT-S tissues. Among the top downregulated miRNAs, the expression of miR-150-5p, miR-342-3p and miR-142-3p positively correlated with each other in PCa patients according to TCGA data (Fig. S1A). Therefore, we chose the three miRNAs for further study. To validate the expression level of the three miRNAs in NHT-R PCa, RT-qPCR was performed in patients who had received NHT in the Qilu cohort. As shown in Fig. 1C-E, expression levels of the three miRNAs were significantly downregulated in NHT-R group, compared with those of NHT-S tissues. Importantly, receiver operating characteristic (ROC) curve demonstrated that the three miRNAs could clearly separate the NHT-R and NHT-S patients, with the area under curve (AUC) of 0.839, 0.799 and 0.760, respectively (Fig. 1F-H, $P < 0.01$). Bioinformatics analysis showed that the enrichment score of miRNAs target signature were higher in NHT-R samples than NHT-S ones, indicating lower miRNAs expression in NHT-R samples according to Tewari cohort [33] (Fig. 1I). The relevance of miR-142-3p and miR-342-3p with bicalutamide resistance was also confirmed in GSE66035 data (Fig. 1J-K). In addition, we also found lower expression of the three miRNAs in tumors with Gleason score ≥ 8 than those of tumors with Gleason score < 8 (Fig. S1B-D, $P < 0.05$ or $P < 0.01$). These findings suggest that decreased expression of the three miRNAs may be responsible for resistance to NHT regimen of PCa patients.

miR-142-3p, miR-150-5p and miR-342-3p attenuate antiandrogen resistance in vitro

To determine the role of the three miRNAs in PCa cells, we firstly compared the expression of the three miRNAs in androgen responsive

LNCAp, VCaP cells and NHT-R cell line 22RV1 and LNCAp-ENZr. Expression of miRNAs in LNCAp-ENZr was significantly lower than that of the parental LNCAp cell line. Of note, the 22RV1 cell line, with deviant expression of AR-V7, failed to demonstrate low expression of three miRNAs (Fig. S2A-C). MTS (Fig. 2A-D) assay and EdU (Fig. S2D) assay demonstrated that these three miRNAs mimics significantly inhibited proliferation of LNCAp and VCaP cells, whereas transfection with inhibitors of the three miRNAs promoted proliferation of PCa cells ($P < 0.05$).

MTS assay revealed that the IC50 value of bicalutamide was $44\mu\text{M}$ in LNCAp cells (Fig. S2E). In an attempt to determine whether the three miRNAs regulate antiandrogen therapy resistance, we found that exogenous expression of three miRNAs increased sensitivity of LNCAp cells to bicalutamide (Fig. 2E-G). In addition, transfection of miRNA mimics strengthened the inhibitory effects of bicalutamide to LNCAp cells, while transfection of inhibitors alleviated the suppressive effects of bicalutamide (Fig. 2H-N, S2F). Similar results were observed in NHT-R LNCAp-ENZr and 22RV1 cells when treated with enzalutamide (Fig. 2O-P). These data indicated that the three miRNAs could attenuate antiandrogen resistance *in vitro*.

CREB5 is the direct target of miR-142-3p, miR-150-5p and miR-342-3p

Dysregulation of AR signaling is one of the major mechanisms that drive NHT-R of PCa. As shown in Fig. 3A-D, transfection of three miRNAs mimics in LNCAp-ENZr and 22RV1 cells downregulated mRNA levels of AR and AR target gene PSA, while transfection of the miRNA inhibitors increased the mRNA expression of AR and PSA. GSEA analysis with TCGA data also revealed the negative correlation of miRNAs with AR signaling (Fig. 3E). However, AR was not identified as target gene of miRNAs according to prediction algorithms (MiRWalk, miranda, RNA22 and Targetscan). To characterize the molecular mechanism by which the three miRNAs promote antiandrogen resistance, a total of 16 potential common targets were predicted on cross-comparison of four prediction algorithms (MiRWalk, miranda, RNA22 and Targetscan) (Fig. 3F). Of note, three of 16 genes, CREB5, AFF1 and CFLAR, were upregulated in NHT-R tissue according to Tewari cohort (Fig. 3G). We further validated the expression of CREB5, AFF1 and CFLAR in our LNCAp/LNCAp-ENZr cell line. RT-qPCR results showed that CREB5 was the most upregulated gene in LNCAp-ENZr cell line (Fig. S2G).

To verify whether the expression of CREB5 was actually regulated by the three miRNAs, we evaluated the expression level of CREB5 after transfection with mimics or inhibitor of these miRNAs in PCa cells. RT-qPCR (Fig. S2H) and Western blot assays (Fig. 3H) revealed that exogenous expression of the three miRNAs significantly reduced both mRNA and protein levels of CREB5 in LNCAp cells. By contrast, inhibitors of the three miRNAs enhanced CREB5 expression (Fig. 3I, S2I). The predicted 3'-UTR sequence of CREB5 that interacted with the three miRNAs was shown in Fig. 3J-K, in which the three recognizing regions of miR-142-3p, two of miR-150-5p and one of miR-342-3p were included. To determine whether this effect was direct, we assayed luciferase reporter gene expression in HEK-293T cells co-transfected with a pmirGLO-promoter vector carrying the respective wild-type or mutant CREB5 3'UTR and corresponding mimics of miR-142-3p, miR-150-5p, and miR-342-3p. The relative luciferase activity was inhibited by mimics of three miRNAs, and such effects were not observed when treated with the mutant construction of CREB5 3'UTR (Fig. 3L-N).

CREB5 promotes proliferation of PCa cells

To perform gain- and loss- function analyses *in vitro*, the expression of CREB5 in PCa cells and transfection efficiency were shown in Fig. S3A-E. MTS (Fig. 4A-B) and EdU (Fig. 4C-D) assays revealed that CREB5 overexpression resulted in significantly increased proliferation, while CREB5 knockdown inhibited cells proliferation activity. Colony formation assay (Fig. S3F) showed enhanced clonogenicity of LNCAp cells by CREB5 overexpression ($P < 0.05$).

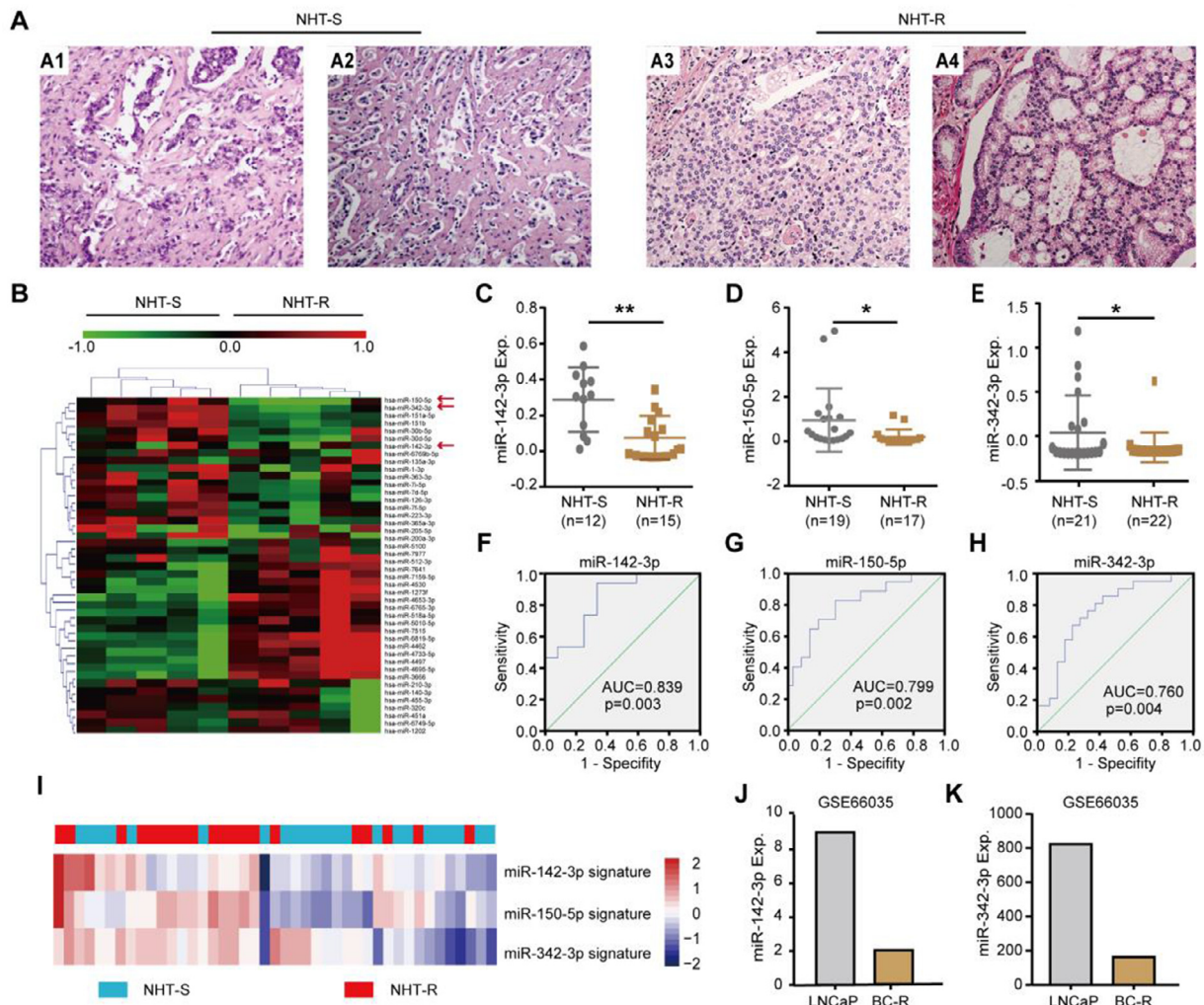


Fig. 1. MiR-142-3p, miR-150-5p and miR-342-3p are downregulated in PCA tissues with NHT-R and associated with high Gleason score. (A) Representative HE images of RP tissues of PCA with NHT-S and NHT-R. Morphological images of NHT-S patients - showing significantly reduced tumor cellularity (A1-A2). Morphological images of intrinsic NHT-R cases - showing no identifiable reduction of tumor cells (A3-A4). (B) Hierarchical clustering of PCA samples in NHT-S ($n = 5$) and NHT-R ($n = 5$) groups on the basis of differentially expressed miRNAs. Each row represents the expression level of an individual miRNA, and each column represents an individual tissue sample. (C-E) Expression of miR-142-3p, miR-150-5p and miR-342-3p in PCA biopsy tissues with NHT-S or NHT-R in Qilu cohort. (F-H) ROC curve showing sensitivity and specificity of miRNAs expression predicting NHT-R. (I) Enrichment score of signatures composed of target genes of miRNAs in NHT-S and NHT-R samples according to Tewari cohort. The signatures composed of target genes of miRNAs were downloaded from MsigDB of GSEA (<http://www.gseamsigdb.org/gsea/msigdb/index.jsp>). Enrichment score were quantified by ssGSEA in R package GSVA. (J-K) Expression of miR-142-3p, miR-342-3p in LNCaP and bicalutamide resistant LNCaP cells in GSE66035. Original magnification of H&E images, $\times 200$. BC-R, bicalutamide resistant. * $P < 0.05$. ** $P < 0.01$.

CREB5 promotes antiandrogen resistance in PCA cells

In an attempt to determine whether CREB5 regulates antiandrogen resistance, we found that CREB5 overexpression significantly decreased sensitivity to bicalutamide in LNCaP cells (Fig. 4E). The IC50 value of bicalutamide was increased by 1.5 times (37.96 vs. 57.16, $P < 0.001$) upon CREB5 overexpression. Enhanced CREB5 expression attenuates the inhibitory effect of bicalutamide on LNCaP cells (Fig. 4F, $P < 0.01$). In addition, exogenous expression of CREB5 blocked the sensitization of miRNAs to bicalutamide and enzalutamide in LNCaP-ENZR and 22RV1 cells, respectively (Fig. 4G-J). RT-qPCR results also revealed that overexpression of CREB5 increased the mRNA expression of AR and PSA upon miRNA mimics transfection (Fig. 4K-L). Taken together, these results indicated that the three miRNAs promote antiandrogen resistance through CREB5 in PCA cells.

IL6 signaling is involved in CREB5-mediated antiandrogen resistance

To study the underlying mechanisms by which CREB5 promotes antiandrogen resistance of PCA cells, we performed GSEA in CREB5 transcriptomes in LNCaP cells with CREB5 overexpression and NHT-R samples in Tewari cohort. We found IL6-JAK-STAT3 signaling pathway genes were significantly enriched both in PCA cells with CREB5 overexpression ($P = 0.018$, $FDR = 0.101$) and NHT-R patients with CREB5 high expression ($P = 0.039$, $FDR = 0.102$) (Fig. 5A-B). Previous studies have revealed that IL6 not only plays an important role in PCA progression but also contributes to CRPC [34,35]. Thereby we hypothesized that IL6 may be involved in this antiandrogen resistant processes. In addition, in silico analysis revealed that the expression of CREB5 was strongly related to IL6 expression in GSE141551 (Fig. 5C, $r = 0.61$, $P < 0.0001$) and TCGA cohort (Fig. 5D, $r = 0.63$, $P < 0.0001$) respectively. Furthermore, exogenous expression of CREB5 could significantly upregulates

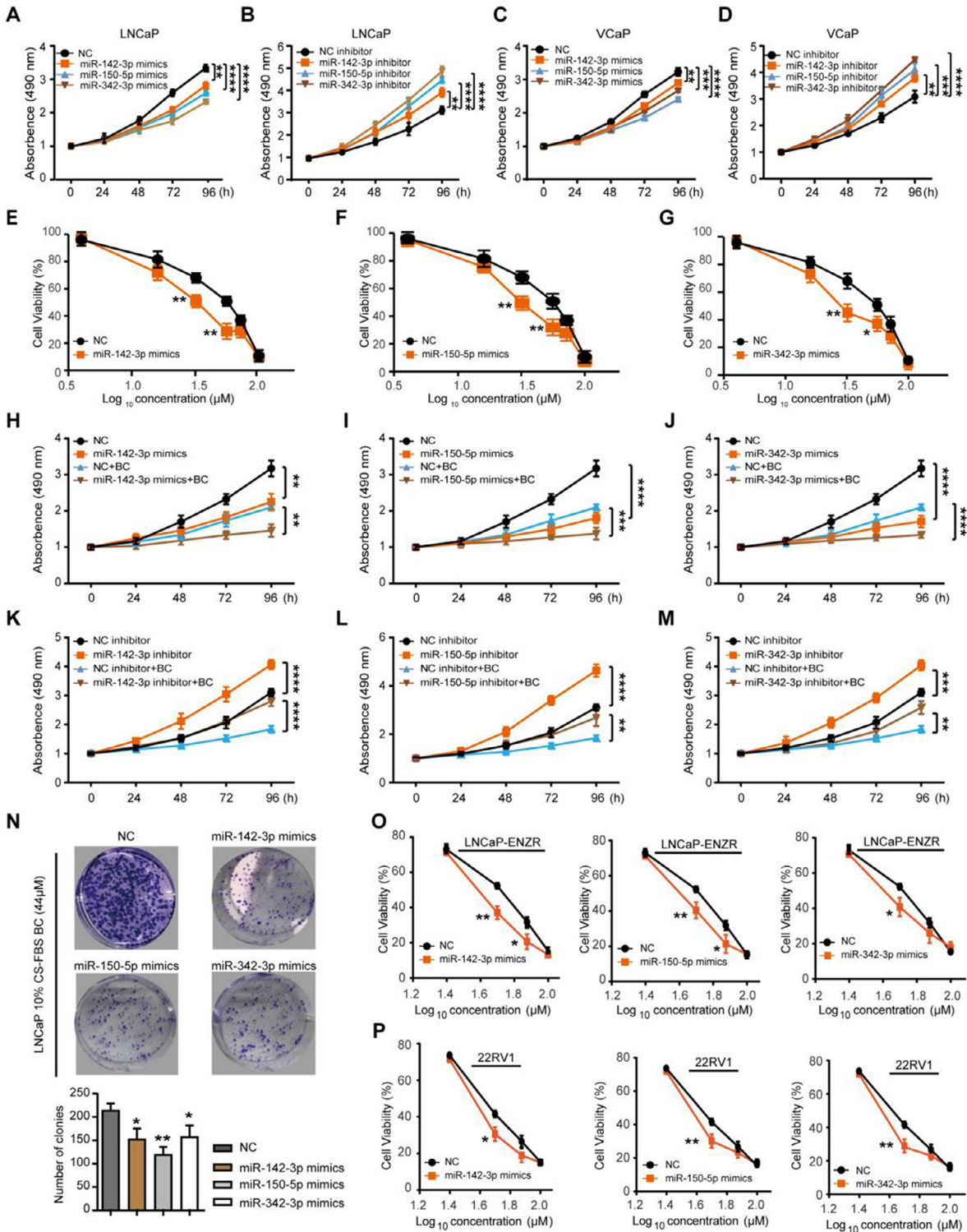


Fig. 2. MiR-142-3p, miR-150-5p and miR-342-3p inhibit proliferation and enhance antiandrogen therapy sensitivity in PCA cells *in vitro*. (A-D) Cell viability assessed by MTS assay at different time points, ranging from 0 to 96h in LNCaP (A-B) and VCaP cells (C-D). (E-G) MTS assays used to quantify cell viability. LNCaP cells cultured with CS-FBS are transiently transfected with indicated miRNAs mimics and treated with titrated dose of bicalutamide for 48 h. (H-M) Cell proliferation determined in indicated LNCaP cells with bicalutamide treatment. LNCaP cells cultured with CS-FBS were transfected with miRNAs mimics/inhibitors as indicated. Following treatment with 44 μM bicalutamide, the cells were subjected to MTS assays. (N) Cell proliferation was assessed by colony formation assay in LNCaP cells transfected with miRNAs mimics with bicalutamide treatment. Cells were cultured for 2 weeks followed by staining with crystal violet and photography. Quantitative analysis of colony numbers is shown in the lower panel. (O-P) IC50 of enzalutamide determination by MTS assays in LNCaP-ENZR and 22RV1 cells. Cells cultured with CS-FBS are transiently transfected with indicated miRNAs mimics and treated with titrated dose of enzalutamide for 48h. **P* < 0.05, ***P* < 0.01, ****P* < 0.001, *****P* < 0.0001. Error bars represent the means ± SD of three independent experiments. BC, bicalutamide. CS-FBS, charcoal-stripped fetal bovine serum.

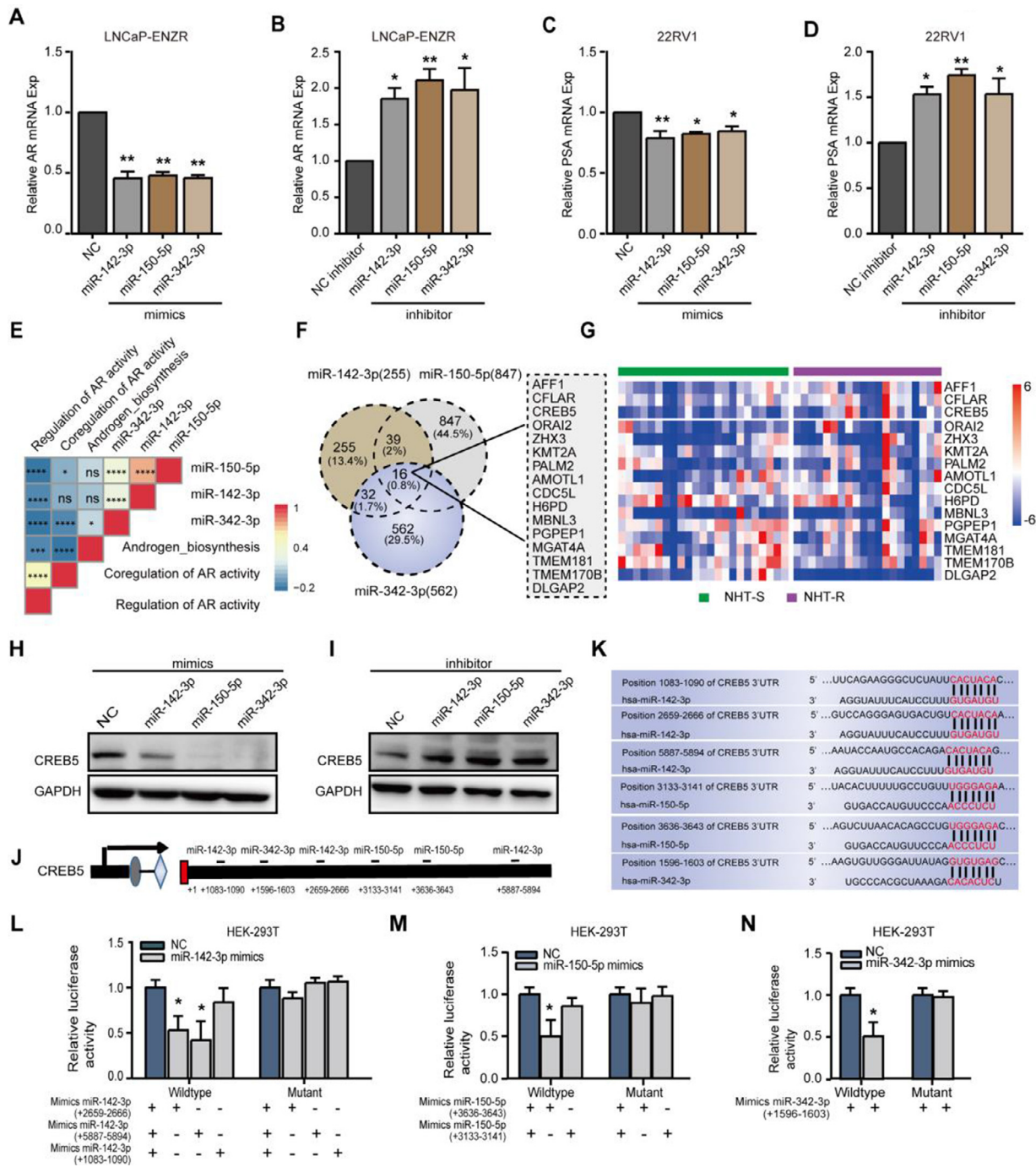


Fig. 3. CREB5 is the direct target of miR-142-3p, miR-150-5p and miR-342-3p. (A-D) The mRNA level of AR and PSA measured in LNCaP-ENZR and 22RV1 cells after transfection with indicated miRNAs mimics/inhibitor (RT-qPCR). (E) Heatmap displaying the relation of enrichment score of AR related signatures with miR-142-3p, miR-150-5p and miR-342-3p expression according to TCGA data. The color represents the correlation coefficient and P-value are reported. The AR related signatures were downloaded from MsigDB of GSEA (<http://www.gsea-msigdb.org/gsea/msigdb/index.jsp>). Enrichment score were quantified by ssGSEA in R package GSVA. (F) A Venn diagram depicted sixteen genes that commonly targeted by indicated miRNAs, which based on four prediction algorithms (MirWalk,miranda,RNA22 and Targetscan). (G) Heatmap displaying the expression of miRNAs target genes in Tewari cohort. (H-I) The protein level of CREB5 assessed in LNCaP cells by Western blot after transfection with indicated miRNAs mimics/inhibitor and relative control RNA. (J-K) The recognition sites for indicated miRNAs in CREB5 3'UTR region. (L-N) Luciferase reporter assay performed in HEK-293T cells. Cells were transiently co-transfected with the wild or mutated CREB5 3'UTR region together with corresponding miRNA mimics, respectively. After incubation for 48h, luciferase activities were measured. * $P < 0.05$, ** $P < 0.01$, *** $P < 0.001$, **** $P < 0.0001$.

the mRNA level of IL6 in LNCaP cells (Fig. 5E, $P < 0.01$). In addition, transfection of miRNAs mimics decreased, while miRNAs inhibitor increased the IL6 level in 22RV1 and LNCaP-ENZR cells (Fig. 5F-I). These results indicated that IL6 signaling may be involved in CREB5-mediated antiandrogen resistance.

CREB5 is highly expressed in Pca tissues with NHT-R

To examine the correlation of CREB5 with NHT-R, we used IHC staining for CREB5 in 85 preoperative needle biopsy samples from Qilu Pca cohort (Table 1). Among the 23 Pca patients with NHT-R, 5 (22%)

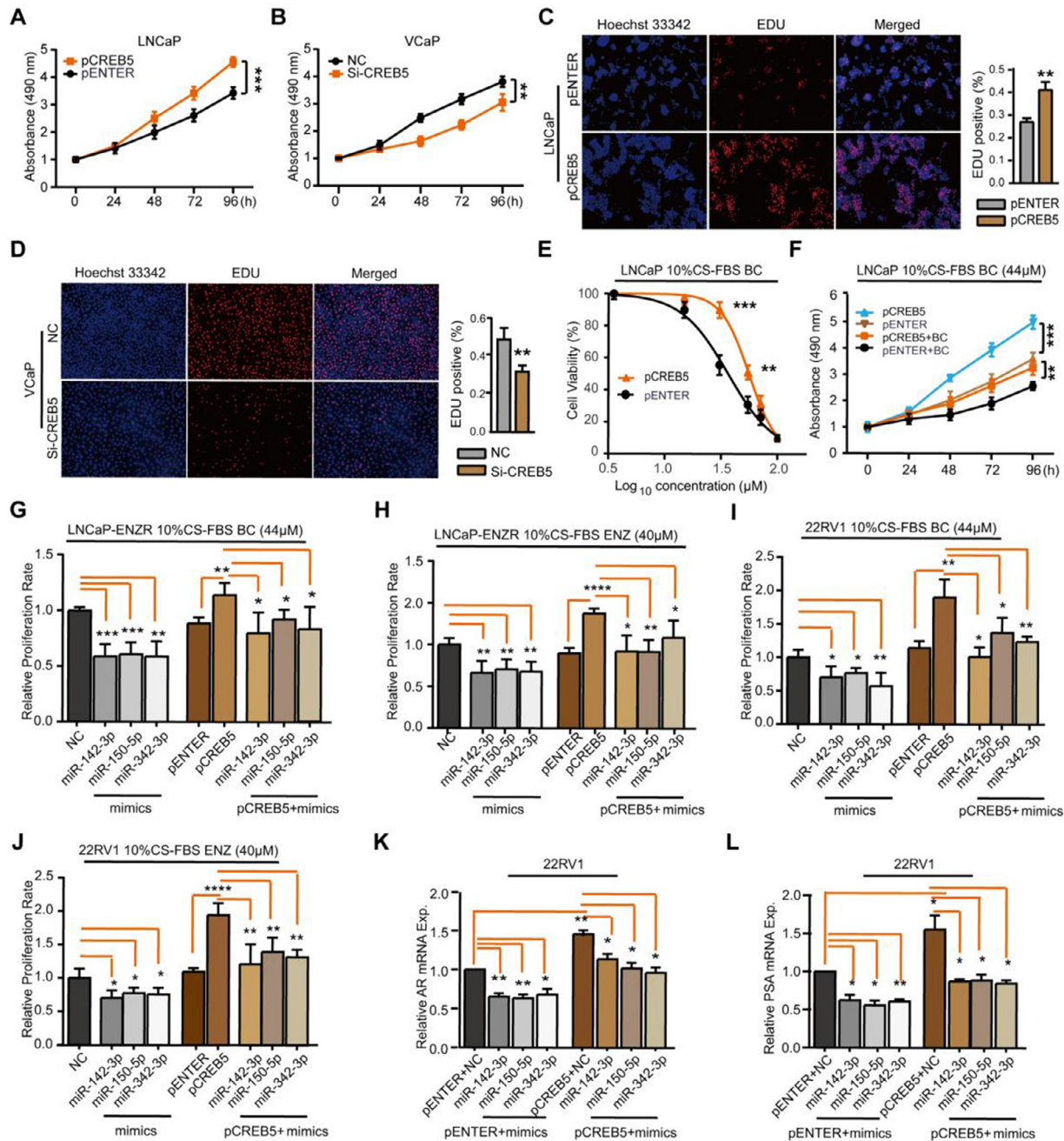


Fig. 4. CREB5 promotes proliferation and antiandrogen resistance *in vitro*. (A-D) Cell proliferation measured in LNCaP and VCaP cells. MTS assays (A-B) and EdU (C-D) assays were performed in LNCaP cells with CREB5 overexpression and in VCaP cells with CREB5 knockdown. Quantitative results of EdU assays are shown in the right panel. (E) Cell viability measured in the LNCaP cells under bicalutamide treatment. LNCaP cells were transfected with CREB5 plasmids/negative control and treated with titrated doses of bicalutamide for 48h. Cell viability was quantified by MTS assays. Data shown are means \pm SD. (F) Cell proliferation determined with bicalutamide treatment. LNCaP cells were transiently transfected with CREB5 overexpression. Following treatment with 44 μ M bicalutamide, the cells were subjected to MTS assays. (G-J) Relative proliferation rate of LNCaP-ENZR (G-H) and 22RV1 cells (I-J). Cells were transfected as indicated, then subjected to MTS assays treated with bicalutamide or enzalutamide. Cells were cultured in 10% CS-FBS. The absorbance at 490nm was measured after 48h treatment with bicalutamide or enzalutamide. (K-L) The mRNA levels of AR(K) and PSA(L) assessed by RT-qPCR after transfection as indicated in 22RV1 cells. * $P < 0.05$, ** $P < 0.01$, *** $P < 0.001$. All data represent means \pm SD of at least three independent replicates.

cases showed negative or weak, whereas 18 (78%) were moderate or strong expression ($P < 0.05$) (Fig. 6A1-A3). These results indicated that CREB5 expression is associated with NHT-R in PCa tissues. Moreover, ROC curves were generated to validate the ability of CREB5 to predict the NHT-R and NHT-S cases with the AUC of 0.674 (Fig. 6B, $P = 0.014$). We also found high CREB5 expression was positively correlated with high Gleason Score (Fig. 6C1-C3) and advanced pathological T stage

($P < 0.01$) (Table 1). ROC curves demonstrated that CREB5 expression could clearly separate and were generated to divide tumors with Gleason < 8 and Gleason ≥ 8 , with the AUC of 0.719 (Fig. 6D, $P = 0.001$). In addition, an inverse correlation between CREB5 and the three miRNAs expression was identified in PCa tissues (Fig. 6E-G), further supporting that the three miRNAs regulate CREB5 expression. Transcriptome analyses of TCGA data revealed that higher levels of CREB5 was proved to be

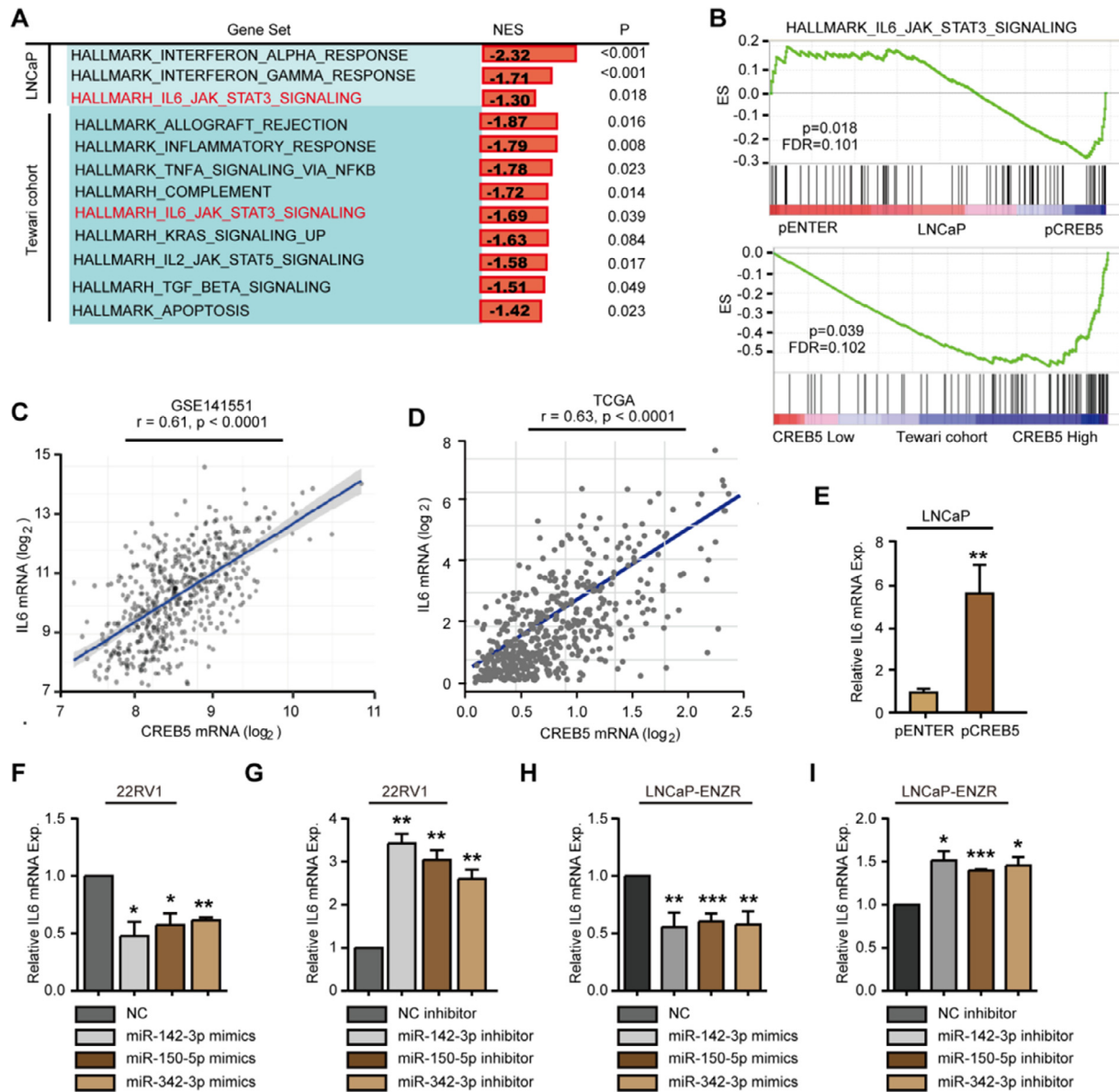


Fig. 5. IL6 signaling is involved in CREB5-mediated antiandrogen resistance. (A-B) Gene sets significantly enriched in high-CREB5 tumors accordingly to the original annotation in the MsigDB Database Hallmark (<http://software.broadinstitute.org/gsea/msigdb/index.jsp>). Normalized enrichment score (NES) and P-value (P) are reported. (C-D) Correlation between the mRNA levels of CREB5 and IL6 in the GSE141551 (C) and TCGA data (D). Spearman r score and P value are shown. (E) The mRNA levels of IL6 assessed by RT-qPCR after transfection with CREB5 plasmids in LNCaP cells. (F-I) The mRNA levels of IL6 assessed by RT-qPCR after transfection with miRNAs mimics and inhibitors in 22RV1 (F-G) and LNCaP-ENZR (H-I) cells. * $P < 0.05$, ** $P < 0.01$.

correlated with high Gleason score (Fig. 6H) ($P < 0.001$), advanced clinical stage (Fig. 6I) ($P < 0.05$ or $P < 0.01$), pathological stage (Fig. 6J) ($P < 0.001$), and positive lymph node metastasis (Fig. 6K) ($P < 0.05$). We also found a significant gradual increase of CREB5 expression from benign prostatic tissue via primary PCa tissues to metastasis (Fig. 6L, $P < 0.05$ or $P < 0.01$) (MSKCC). Significantly, patients with CREB5 high expression had worse disease-free survival (Fig. 6M, $P = 0.024$) (MSKCC) and biochemical recurrence-free survival (Fig. 6N, $P = 0.002$) (GSE116918). These results suggest that CREB5 could be as a predictive biomarker in antiandrogen resistance and aggressive biological behavior in PCa.

Discussion

HRPCa under NHT regimen have variable outcomes. Despite robust targeting androgen axis, the pathologic complete response to NHT was observed in less than 30% HRPCa patients [7]. Therefore, a subset of patients who do not respond well to hormonal therapy may warrant

alternative treatment strategies. The aim of this study was to evaluate the underlying mechanisms of NHT-R in these patients. Using miRNA microarray analysis of PCa tissues with NHT-R and NHT-S, we identified a group of miRNA predictors of response to NHT for the first time. More importantly, we built a linkage between a trio of tumor suppressor miRNA (miR-142-3p, miR-150-5p and miR-342-3p) and NHT response in PCa patients. Of note, these miRNAs showed prognostic value for NHT response. Based on these findings, our study provides a general view of the concept that miRNAs can directly regulate NHT response in PCa.

Thus far, to the best of our knowledge, multiple evidences have indicated that miRNAs play important roles in treatment resistance and emerged as treatment response predictor of various cancer [36]. It has been reported that high level of miR-621 predicts pathological complete response to paclitaxel plus carboplatin regimen neoadjuvant chemotherapy in breast cancer patients [37]. Elrasheid et. al. reported a miRNAs signature, including miR-16 etc, to predict response to neoadjuvant chemoradiation therapy in rectal cancer [38]. Moreover, Yukiko et. al

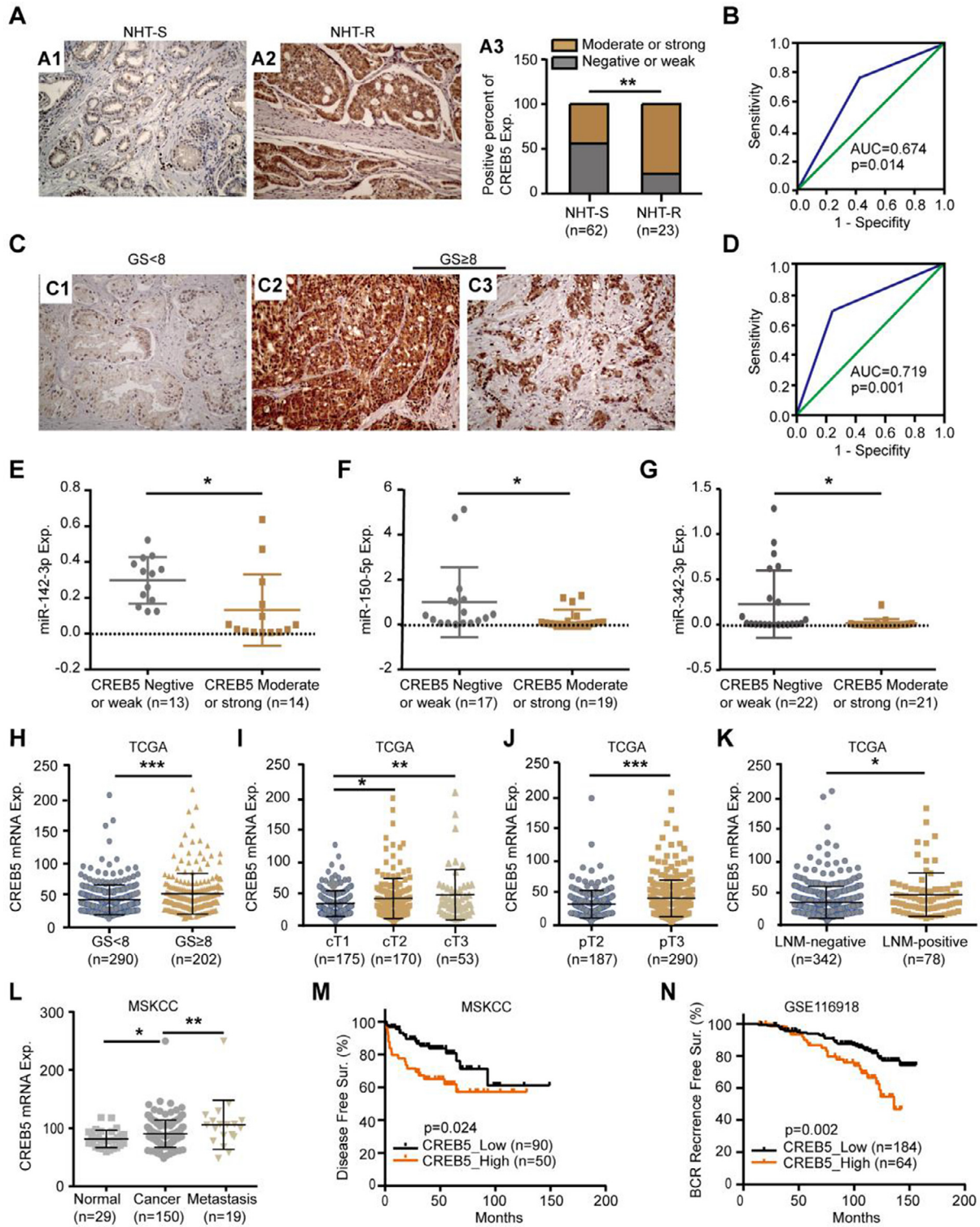


Fig. 6. CREB5 is highly expressed in NHT-R PCA tissues. (A-D) CREB5 expression measured by IHC assay in Qilu cohort. Representative IHC images of CREB5 expression in PCA biopsy tissues with NHT-S (A1) or NHT-R (A2) in Qilu cohort. Quantitative analysis of cases with CREB5 positive was shown in A3. ROC curve was constructed to validate the sensitivity and specificity of CREB5 in predicting NHT-R (B). Representative IHC images of CREB5 expression in cases with Gleason score <8 (C1), and Gleason score ≥8 (C2-C3). ROC curve was constructed to validate the sensitivity and specificity of CREB5 in predicting GS (D). (E-G) The relevance between CREB5 and the three miRNAs expression in Qilu cohort. (H-K) Analysis of CREB5 expression in TCGA dataset. (H) CREB5 levels in PCA subgroups with different Gleason scores; (I) CREB5 levels in PCA subgroups with different clinical stages; (J) CREB5 levels in PCA subgroups with different pathological stages; (K) CREB5 levels in PCA subgroups with lymph node metastasis. (L-M) Analysis of CREB5 expression in MSKCC dataset. (L) The expression of CREB5 in primary and metastatic PCA tissues compared with the matched normal prostate samples in MSKCC dataset. (M) The correlation between CREB5 expression and biochemical recurrence-free survival in MSKCC cohort (Kaplan–Meier survival, Log-rank test). (N) The correlation between CREB5 expression and biochemical recurrence-free survival in GSE116918 data (Kaplan–Meier survival, Log-rank test). TCGA The Cancer Genome Atlas. GS, Gleason score. cT, clinical stage. pT, pathological stage. LNM, lymph node metastasis. BCR, biochemical recurrence. Error bars represent means ± SD of three independent experiments. Original magnification of IHC images, × 200. *P < 0.05.

Table 1
Clinicopathological analysis for CREB5 by immunohistochemistry in 85 PCa patients.

Variables	n	CREB5 expression		P-value
		Negative or weak	Moderate or strong	
Age (yr) Median (range)	85	68(47-79)	70(57-78)	
Therapy Status				0.007
NHT-S	62	35	27	
NHT-R	23	5	18	
Pre-operative PSA (ng/ml)				0.156
≤10	15	10	5	
10-20	17	10	7	
>20	53	20	33	
Pre-operative Gleason Score				0.000
<8	29	22	7	
≥8	56	18	38	
Surgical Margins				0.292
Positive	26	10	16	
Negative	59	30	29	
Pathologic Stage				0.004
p≤T2	50	30	20	
pT3	35	10	25	

PCa, prostate cancer; NHT, neoadjuvant hormonal therapy; PSA, prostate specific antigen.

identified a serum miRNAs signature for response of esophageal squamous cell carcinoma to neoadjuvant therapy [39]. In the current study, we found that high expression of a trio of tumor suppressor miRNA in PCa patients predict better pathologic response to NHT. Previously, the non-invasive detection of miR-150-5p and miR-142-3p as biomarkers of PCa has been illustrated elsewhere [40,41]. Therefore, our new finding not only highlighted the role of miRNAs in NHT-R of PCa for the first time, but also provided possibility of non-invasive detection to screen patients suitable for NHT.

Resistant mechanisms against hormonal therapy in CRPC progression has been extensively explored, including AR based aberrations and genomic alterations of other oncogenes. However, the underlying mechanisms of CRPC and intrinsic NHT-R might be different, because of far less mutagenic genomic feature of localized PCa when NHT regimens were used. So far, possible resistance mechanisms to NHT before RP in HRPCa are unclear. The pathology responses to NHT did not trend with classical clinicopathological features, such as clinical stage and Gleason score, although the presence of intraductal carcinoma of PCa were predictive of poor response to NHT [42]. Recent studies indicated the value of genomic biomarkers, including PTEN loss, TP53 mutation and ERG expression in distinguishing exceptional responders from poor responders to NHT [42]. Our previous study also revealed that PTEN loss could be as a biomarker to predict response to NHT in HRPCa patients [10]. Here, we found high level expression of CREB5 in NHT-R tumors. Increased CREB5 expression results in bicalutamide resistance in PCa cells due to down-regulation of miR-142-3p, miR-150-5p and miR-342-3p. Results of Western blot assays in PCa cells and luciferase report assays in HEK-293T cells further validated CREB5 as direct target of the three miRNAs.

CREB5 is a transcription factor [43] overexpressed in various types of human malignancies, such as carcinoma of the colon [44], ovary [45] and liver [46]. Previously, Justin et. al reported that CREB5 interacted with AR and sustained AR transcriptional program in the presence of FOXA1 which resulted in CRPC [25]. In the current study, we found the positive correlation of CREB5 and IL6-STAT3 pathway in PCa. It is well known that IL6 is a key mediator in progression of PCa, including metastasis, chemotherapy resistance, and development of CRPC [35]. Enhanced expression of IL-6 was frequently observed after androgen deprivation and castration resistance in clinical setting [47]. Several studies showed that IL-6 activates AR expression and transcriptional activity through STAT3 dependent pathway [48,49]. Overexpression of IL-6 enhanced PSA mRNA expression and can partially rescue LNCaP cells from

growth arrest induced by androgen deprivation therapy [50]. Based on our results, we suggested that the enhanced expression and function of IL-6 caused by CREB5, might mediate the miR-CREB5 axis in emergence of NHT-R.

Conclusion

MiR-142-3p, miR-150-5p and miR-342-3p are downregulated in PCa tissues with NHT-R and associated with high Gleason score. These three miRNAs inhibit proliferation and enhance bicalutamide sensitivity of PCa cells *in vitro*. Mechanically, CREB5 is the common target of these three miRNAs. miR-142-3p, miR-150-5p, and miR-342-3p contribute to NHT-R via targeting CREB5 in PCa and IL6 signaling pathway may be involved in this process.

List of Supporting Information

- 1 Supplemental Figure and Figure Legend. docx
- 2 Supplemental Table 1. docx Sequences of miRNA mimics and inhibitor used in this study.
- 3 Supplemental Table 2. docx Sequences of primers employed in this study.

Declaration of Competing Interest

The authors declare that they have no known competing financial interests or personal relationships that could have appeared to influence the work reported in this paper.

CRedit authorship contribution statement

Xueli Wang: Investigation, Validation, Methodology, Software, Writing – review & editing. **Bo Han:** Conceptualization, Software, Supervision, Funding acquisition. **Baokai Dou:** Software, Validation. **Lin Gao:** Methodology, Visualization, Investigation. **Feifei Sun:** Data curation, Validation. **Mei Qi:** Software, Validation. **Jing Zhang:** Conceptualization, Writing – review & editing. **Jing Hu:** Conceptualization, Methodology, Software, Writing – review & editing, Funding acquisition.

Acknowledgments

This work was supported by Joint Research Fund of Natural Science, Shandong Province (ZR2019LZL014), National Natural Science Foundation of China (Grant No. 81972416, 82172818), The Fundamental Research Funds of Shandong University (2018JC016), and Shandong Provincial Natural Science Foundation (ZR2020QH243).

Supplementary materials

Supplementary material associated with this article can be found, in the online version, at doi:10.1016/j.neo.2022.100875.

References

- [1] M.D. Shelley, S. Kumar, T. Wilt, J. Staffurth, B. Coles, M.D. Mason, A systematic review and meta-analysis of randomised trials of neo-adjuvant hormone therapy for localised and locally advanced prostate carcinoma, *Cancer Treat. Rev.* 35 (2009) 9–17.
- [2] I.J. Powell, C.M. Tangen, G.J. Miller, B.A. Lowe, G. Haas, P.R. Carroll, M.B. Osswald, V.W.R. De, I.M. Thompson Jr., E.D. Crawford, Neoadjuvant therapy before radical prostatectomy for clinical T3/T4 carcinoma of the prostate: 5-year followup, Phase II Southwest Oncology Group Study 9109, *J. Urol.* 168 (2002) 2016–2019.
- [3] R.K. Berglund, C.M. Tangen, I.J. Powell, B.A. Lowe, G.P. Haas, P.R. Carroll, E.D. Canby-Hagino, R. de Vere White, G.P. Hemstreet 3rd, E.D. Crawford, et al., Ten-year follow-up of neoadjuvant therapy with goserelin acetate and flutamide before radical prostatectomy for clinical T3 and T4 prostate cancer: update on Southwest Oncology Group Study 9109, *Urology* 79 (2012) 633–637.
- [4] L. Tosco, A. Laenen, A. Briganti, P. Gontero, R.J. Karnes, M. Albersen, P.J. Bastian, P. Chlosta, F. Claessens, F.K. Chun, et al., The survival impact of neoadjuvant hormonal therapy before radical prostatectomy for treatment of high-risk prostate cancer, *Prostate Cancer Prostatic Dis.* 20 (2017) 407–412.
- [5] M.E. Taplin, B. Montgomery, C.J. Logothetis, G.J. Bubley, J.P. Richie, B.L. Dalkin, M.G. Sanda, J.W. Davis, M. Loda, L.D. True, et al., Intense androgen-deprivation therapy with abiraterone acetate plus leuprolide acetate in patients with localized high-risk prostate cancer: results of a randomized phase II neoadjuvant study, *J. Clin. Oncol.* 32 (2014) 3705–3715.
- [6] B. Montgomery, M.S. Tretiakova, A.M. Joshua, M.E. Gleave, N. Fleshner, G.J. Bubley, E.A. Mostaghel, K.N. Chi, D.W. Lin, M. Sanda, et al., Neoadjuvant enzalutamide prior to prostatectomy, *Clin. Cancer Res.* 23 (2017) 2169–2176.
- [7] R.R. McKay, H. Ye, W. Xie, R. Lis, C. Calagua, Z. Zhang, Q.D. Trinh, S.L. Chang, L.C. Harshman, A.E. Ross, et al., Evaluation of intense androgen deprivation before prostatectomy: a randomized Phase II trial of enzalutamide and leuprolide with or without abiraterone, *J. Clin. Oncol.* 37 (2019) 923–931.
- [8] R.R. McKay, J. Berchuck, L. Kwak, W. Xie, R. Silver, G.J. Bubley, P.K. Chang, A. Wagner, Z. Zhang, A.S. Kibel, et al., Outcomes of post-neoadjuvant intense hormone therapy and surgery for high risk localized prostate cancer: results of a pooled analysis of contemporary clinical trials, *J. Urol.* 205 (2021) 1689–1697.
- [9] G. Devos, W. Devlies, G. De Meerleer, M. Baldewijns, T. Gevaert, L. Moris, D. Milonas, H. Van Poppel, C. Berghen, W. Everaerts, et al., Neoadjuvant hormonal therapy before radical prostatectomy in high-risk prostate cancer, *Nat. Rev. Urol.* 18 (2021) 739–762.
- [10] X. Wang, M. Qi, J. Zhang, X. Sun, H. Guo, Y. Pang, Q. Zhang, X. Chen, R. Zhang, Z. Liu, et al., Differential response to neoadjuvant hormonal therapy in prostate cancer: Predictive morphological parameters and molecular markers, *Prostate* 79 (2019) 709–719.
- [11] W. Si, J. Shen, H. Zheng, W. Fan, The role and mechanisms of action of microRNAs in cancer drug resistance, *Clin Epigenet.* 11 (2019) 25.
- [12] S. Haenisch, I. Cascorbi, miRNAs as mediators of drug resistance, *Epigenomics* 4 (2012) 369–381.
- [13] E. Giovannetti, A. Erozcenci, J. Smit, R. Danesi, G.J. Peters, Molecular mechanisms underlying the role of microRNAs (miRNAs) in anticancer drug resistance and implications for clinical practice, *Crit. Rev. Oncol. Hematol.* 81 (2012) 103–122.
- [14] L. Fattore, C.F. Ruggiero, M.E. Pisanu, D. Liguoro, A. Cerri, S. Costantini, F. Capone, M. Acunzo, G. Romano, G. Nigita, et al., Reprogramming miRNAs global expression orchestrates development of drug resistance in BRAF mutated melanoma, *Cell Death Differ.* 26 (2019) 1267–1282.
- [15] X. Chen, Y.W. Wang, A.Y. Xing, S. Xiang, D.B. Shi, L. Liu, Y.X. Li, P. Gao, Suppression of SPIN1-mediated PI3K-Akt pathway by miR-489 increases chemosensitivity in breast cancer, *J. Pathol.* 239 (2016) 459–472.
- [16] C.E. Fletcher, E. Sulpice, S. Combe, A. Shibakawa, D.A. Leach, M.P. Hamilton, S.L. Chrysostomou, A. Sharp, J. Welti, W. Yuan, et al., Androgen receptor-modulatory microRNAs provide insight into therapy resistance and therapeutic targets in advanced prostate cancer, *Oncogene* 38 (2019) 5700–5724.
- [17] K.P. Porkka, M.J. Pfeiffer, K.K. Waltering, R.L. Vessella, T.L. Tammela, T. Visakorpi, MicroRNA expression profiling in prostate cancer, *Cancer Res.* 67 (2007) 6130–6135.
- [18] S. Ams, R.L. Prueitt, M. Yi, R.S. Hudson, T.M. Howe, F. Petrocchi, T.A. Wallace, C.G. Liu, S. Volinia, G.A. Calin, et al., Genomic profiling of microRNA and messenger RNA reveals deregulated microRNA expression in prostate cancer, *Cancer Res.* 68 (2008) 6162–6170.
- [19] P. Gandellini, M. Folini, N. Zaffaroni, Emerging role of microRNAs in prostate cancer: implications for personalized medicine, *Discov. Med.* 9 (2010) 212–218.
- [20] M. Ozen, C.J. Creighton, M. Ozdemir, M. Ittmann, Widespread deregulation of microRNA expression in human prostate cancer, *Oncogene* 27 (2008) 1788–1793.
- [21] B. Kumar, S. Khaleghzadegan, B. Mears, K. Hatano, T.A. Kudrolli, W.H. Chowdhury, D.B. Yeater, C.M. Ewing, J. Luo, W.B. Isaacs, et al., Identification of miR-30b-3p and miR-30d-5p as direct regulators of androgen receptor signaling in prostate cancer by complementary functional microRNA library screening, *Oncotarget* 7 (2016) 72593–72607.
- [22] J. Ribas, X. Ni, M. Haffner, E.A. Wentzel, A.H. Salmasi, W.H. Chowdhury, T.A. Kudrolli, S. Yegnasubramanian, J. Luo, R. Rodriguez, et al., miR-21: an androgen receptor-regulated microRNA that promotes hormone-dependent and hormone-independent prostate cancer growth, *Cancer Res.* 69 (2009) 7165–7169.
- [23] X. Li, M. Jiao, J. Hu, M. Qi, J. Zhang, M. Zhao, H. Liu, X. Xiong, X. Dong, B. Han, miR-30a inhibits androgen-independent growth of prostate cancer via targeting MYBL2, FOXD1, and SOX4, *Prostate* 80 (2020) 674–686.
- [24] H. Liu, Z. Wu, H. Zhou, W. Cai, X. Li, J. Hu, L. Gao, T. Feng, L. Wang, X. Peng, et al., The SOX4/miR-17-92/RB1 axis promotes prostate cancer progression, *Neoplasia* 21 (2019) 765–776.
- [25] J.H. Hwang, J.H. Seo, M.L. Beshiri, S. Wankowicz, D. Liu, A. Cheung, J. Li, X. Qiu, A.L. Hong, G. Botta, et al., CREB5 promotes resistance to androgen-receptor antagonists and androgen deprivation in prostate cancer, *Cell Rep.* 29 (2019) 2355–2370 e2356.
- [26] J.H. Hwang, R. Arafteh, J.H. Seo, S.C. Baca, M. Ludwig, T.E. Arnoff, L. Sawyer, C. Richter, S. Tape, H.E. Bergom, et al., CREB5 reprograms FOXA1 nuclear interactions to promote resistance to androgen receptor-targeting therapies, *Elife* (2022) 11.
- [27] J. Guo, Y. Miao, B. Xiao, R. Huan, Z. Jiang, D. Meng, Y. Wang, Differential expression of microRNA species in human gastric cancer versus non-tumorous tissues, *J. Gastroenterol. Hepatol.* 24 (2009) 652–657.
- [28] F. Sun, X. Wang, J. Hu, J. Liu, X. Wang, W. Jia, Z. Yu, L. Gao, B. Dou, R. Zhao, et al., RUVBL1 promotes enzalutamide resistance of prostate tumors through the PLXNA1-CRAF-MAPK pathway, *Oncogene* 41 (2022) 3239–3250.
- [29] L. Gao, W. Zhang, J. Zhang, J. Liu, F. Sun, H. Liu, J. Hu, X. Wang, X. Wang, P. Su, et al., KIF15-mediated stabilization of AR and AR-V7 contributes to enzalutamide resistance in prostate cancer, *Cancer Res.* 81 (2021) 1026–1039.
- [30] M. Qi, J. Hu, Y. Cui, M. Jiao, T. Feng, X. Li, Y. Pang, X. Chen, R. Qin, P. Su, et al., CUL4B promotes prostate cancer progression by forming positive feedback loop with SOX4, *Oncogenesis* 8 (2019) 23.
- [31] L. Wang, G. Song, X. Zhang, T. Feng, J. Pan, W. Chen, M. Yang, X. Bai, Y. Pang, J. Yu, et al., PAD12-mediated citrullination promotes prostate cancer progression, *Cancer Res.* 77 (2017) 5755–5768.
- [32] M. Qi, M. Jiao, X. Li, J. Hu, L. Wang, Y. Zou, M. Zhao, R. Zhang, H. Liu, J. Mi, et al., CUL4B promotes gastric cancer invasion and metastasis-involvement of upregulation of HER2, *Oncogene* 37 (2018) 1075–1085.
- [33] A.K. Tewari, A.T.M. Cheung, J. Crowdis, J.R. Conway, S.Y. Camp, S.A. Wankowicz, D.G. Livitz, J. Park, R.T. Lis, A. Bosma-Moody, et al., Molecular features of exceptional response to neoadjuvant anti-androgen therapy in high-risk localized prostate cancer, *Cell Rep.* 36 (2021) 109665.
- [34] S. Feng, Q. Tang, M. Sun, J.Y. Chun, C.P. Evans, A.C. Gao, Interleukin-6 increases prostate cancer cells resistance to bicalutamide via TIF2, *Mol. Cancer Ther.* 8 (2009) 665–671.
- [35] D.P. Nguyen, J. Li, A.K. Tewari, Inflammation and prostate cancer: the role of interleukin 6 (IL-6), *BJU Int.* 113 (2014) 986–992.
- [36] L. Mulrane, S.F. McGee, W.M. Gallagher, D.P. O'Connor, miRNA dysregulation in breast cancer, *Cancer Res.* 73 (2013) 6554–6562.
- [37] J. Xue, Y. Chi, Y. Chen, S. Huang, X. Ye, J. Niu, W. Wang, L.M. Pfeiffer, Z.M. Shao, Z.H. Wu, et al., miRNA-621 sensitizes breast cancer to chemotherapy by suppressing FBXO11 and enhancing p53 activity, *Oncogene* 35 (2016) 448–458.
- [38] E.A. Kheirlelid, N. Miller, K.H. Chang, C. Curran, E. Hennessey, M. Sheehan, J. Newell, C. Lemetre, G. Balls, M.J. Kerin, miRNA expressions in rectal cancer as predictors of response to neoadjuvant chemoradiation therapy, *Int. J. Colorectal Dis.* 28 (2013) 247–260.
- [39] Y. Niwa, S. Yamada, F. Sonohara, K. Kurimoto, M. Hayashi, M. Tashiro, N. Iwata, M. Kanda, C. Tanaka, D. Kobayashi, et al., Identification of a serum-based miRNA signature for response of esophageal squamous cell carcinoma to neoadjuvant chemotherapy, *J. Transl. Med.* 17 (2019) 1.
- [40] I.A. Paunescu, R. Bardan, A. Marcu, D. Nitusca, A. Dema, S. Negru, O. Balacescu, L. Balacescu, A. Cumpanas, I.O. Sirbu, et al., Biomarker potential of plasma MicroRNA-150-5p in prostate cancer, *Medicina* (2019) 55 (Kaunas).
- [41] M. Barcelo, M. Castells, M. Perez-Riba, L. Bassas, F. Vignes, S. Larrriba, Seminal plasma microRNAs improve diagnosis/prognosis of prostate cancer in men with moderately altered prostate-specific antigen, *Am. J. Transl. Res.* 12 (2020) 2041–2051.
- [42] S. Wilkinson, H. Ye, F. Karzai, S.A. Harmon, N.T. Terrigino, D.J. Vanderweele, J.R. Bright, R. Atway, S.Y. Trostel, N.V. Carrabba, et al., Nascent prostate cancer heterogeneity drives evolution and resistance to intense hormonal therapy, *Eur. Urol.* (2021).
- [43] N. Nomura, Y.L. Zu, T. Maekawa, S. Tabata, T. Akiyama, S. Ishii, Isolation and characterization of a novel member of the gene family encoding the cAMP response element-binding protein CRE-BP1, *J. Biol. Chem.* 268 (1993) 4259–4266.
- [44] L. Qi, Y. Ding, Involvement of the CREB5 regulatory network in colorectal cancer metastasis, *Yi Chuan* 36 (2014) 679–684.
- [45] S. He, Y. Deng, Y. Liao, X. Li, J. Liu, S. Yao, CREB5 promotes tumor cell invasion and correlates with poor prognosis in epithelial ovarian cancer, *Oncol. Lett.* 14 (2017) 8156–8161.

- [46] J. Wu, S.T. Wang, Z.J. Zhang, Q. Zhou, B.G. Peng, CREB5 promotes cell proliferation and correlates with poor prognosis in hepatocellular carcinoma, *Int. J. Clin. Exp. Pathol.* 11 (2018) 4908–4916.
- [47] A. Hobisch, I.E. Eder, T. Putz, W. Horninger, G. Bartsch, H. Klocker, Z. Culig, Interleukin-6 regulates prostate-specific protein expression in prostate carcinoma cells by activation of the androgen receptor, *Cancer Res.* 58 (1998) 4640–4645.
- [48] T. Chen, L.H. Wang, W.L. Farrar, Interleukin 6 activates androgen receptor-mediated gene expression through a signal transducer and activator of transcription 3-dependent pathway in LNCaP prostate cancer cells, *Cancer Res.* 60 (2000) 2132–2135.
- [49] A. Schroeder, A. Herrmann, G. Cherryholmes, C. Kowolik, R. Buettner, S. Pal, H. Yu, G. Muller-Newen, R. Jove, Loss of androgen receptor expression promotes a stem-like cell phenotype in prostate cancer through STAT3 signaling, *Cancer Res.* 74 (2014) 1227–1237.
- [50] S.O. Lee, W. Lou, C.S. Johnson, D.L. Trump, A.C. Gao, Interleukin-6 protects LNCaP cells from apoptosis induced by androgen deprivation through the Stat3 pathway, *Prostate* 60 (2004) 178–186.